NASA Technical Paper 1600



# A Relation Between Semiempirical Fracture Analyses and R-Curves

Thomas W. Orange

JANUARY 1980

NASA

NASA Technical Paper 1600

# A Relation Between Semiempirical Fracture Analyses and R-Curves

Thomas W. Orange
*Lewis Research Center*
*Cleveland, Ohio*

National Aeronautics
and Space Administration

**Scientific and Technical
Information Office**

1980

## SUMMARY

The relations between several semiempirical fracture analyses (SEFA) and the R-curve concept of fracture mechanics are examined and the conditions for equivalence between a SEFA and an R-curve are derived. A hypothetical material is employed to study the relation analytically. Equivalent R-curves are developed for several real materials using data from the literature. For each SEFA there is an equivalent R-curve whose magnitude and shape are determined by the SEFA formulation and its empirical parameters. If the R-curve is indeed unique, then the various empirical parameters cannot be constant, and vice versa. However, for one SEFA the differences are small enough that they may be within the range of normal data scatter for real materials.

## INTRODUCTION

The relations between several semiempirical fracture analyses and the R-curve concept of fracture mechanics are examined. These relations may explain why a semiempirical fracture analysis will yield good results with one set of data and poor results with another. They may also indicate which analyses deserve further consideration.

Over the past decade a number of semiempirical fracture analyses have been presented (refs. 1 to 5). These analyses all attempt to correlate failure stresses for precracked tension specimens with initial crack length over a range of crack lengths. The correlations involve the determination of one (refs. 1 to 3) or two (refs. 4 and 5) empirical parameters from test data. The parameters are treated as material properties which are independent of the specimen and crack configurations but which are functions of specimen thickness and such variables as heat treatment and test temperature. The analyses often provide very good correlations using some data sets but poor correlations using other data sets. To date these analyses have only been formulated for and applied to test specimen configurations. Thus their applicability to the design of complex structural configurations is uncertain.

The progressive development of the R-curve concept has been reviewed in reference 6. The concept postulates that, for a given material and thickness, there is a unique relation between the amount of stable crack growth under rising load and the crack-tip stress intensity factor. This relation is called the crack extension resistance curve, or R-curve, and represents the response of the material in the vicinity of the crack tip to externally imposed loading. If the R-curve is known, both failure load and critical crack length can be predicted (as functions of initial crack length) for any spe-

cimen or structural configuration for which an appropriate stress intensity analysis is available. Thus the R-curve concept appears to be a much more useful method than any of the semiempirical analyses.

If the R-curve for a given material and thickness is available, one can calculate residual strength (fracture stress as a function of initial crack length) for any test specimen configuration. The converse should also be true. That is, if a relation between fracture stress and initial crack length is available, one should be able to calculate the corresponding R-curve. This observation was the impetus for the present study, which was undertaken to test the following hypotheses:

(1) For each semiempirical fracture analysis (SEFA) there is an equivalent R-curve (ERC) whose magnitude and shape are determined by the SEFA formulation and its empirical parameters. The ERC is equivalent in that it predicts exactly the same relation between fracture stress and initial crack length as the SEFA.

(2) A SEFA will correlate residual strength data closely if its ERC closely matches the actual R-curve of the material in question and will correlate poorly if the match is poor.

(3) It should be possible to predict the critical crack length in terms of the initial crack length and the empirical parameters.

This report first reviews some characteristics of the R-curve concept when applied to finite-width specimens. Next the conditions for equivalence between a semiempirical analysis and an R-curve are derived. A hypothetical material is employed to study the relation between R-curves and semiempirical analyses. Finally, equivalent R-curves are developed for several real materials using data from the literature.

## SYMBOLS

| | |
|---|---|
| $a$ | length of single-tip crack or half-length of double-tip crack, $a_o + \Delta$ |
| $B$ | specimen thickness |
| $C_m$ | empirical parameter (ref. 1) |
| $E'$ | effective modulus, $E$ for plane stress or $E/(1 - \nu^2)$ for plane strain, where $E$ is Young's modulus and $\nu$ is Poisson's ratio |
| $G_A$ | strain energy release rate |
| $G_R$ | crack extension resistance |
| $G_c$ | fracture toughness, $G_A$ or $G_R$ at instability condition |
| $K_c$ | empirical parameter (ref. 3) |
| $K_f$ | empirical parameter (ref. 4) |

$K_{Tc}$ empirical parameter (ref. 5)

$K_u$ empirical parameter (ref. 2)

$K_I$ opening-mode stress intensity factor

m empirical parameter (ref. 4)

n number of crack tips (one or two)

W specimen width

Y stress intensity calibration factor, $K_I/\sigma\sqrt{a}$

$\alpha$ sensitivity factor (eq. (1))

$\Delta$ effective crack extension (sum of physical crack extension plus a plastic zone correction)

$\lambda$ relative crack length, na/W

$\sigma$ stress normal to crack

$\sigma_u$ ultimate tensile strength

$\sigma_{ys}$ yield strength

$\omega$ empirical parameter (ref. 5)

Subscripts:

c at critical or instability condition

o initial value (prior to loading)

## R-CURVE CONCEPT

The R-curve concept is illustrated schematically in figure 1 for an infinite body containing a crack whose original length is $2a_o$. The strain energy release rate is given by

$$G_A = \frac{\sigma^2 \pi a}{E'}$$

and represents the driving force (per unit thickness) tending to cause crack propagation. The material's resistance to crack propagation, $G_R$, is a function of crack extension, $\Delta$. In R-curve analysis the subscripts A, R, and c are customarily used to denote applied and resisting forces and critical values, respectively. The R-curve is located with its origin at $a = a_o$. As stress normal to the crack is applied and increased to 90 percent of the subsequent critical stress in figure 1, the crack must extend only a small distance

to develop a large resistance. At this point the crack extension resistance equals the driving force and the crack is stable. As the stress is increased, progressively larger amounts of crack extension are required to resist the crack driving force. Finally, at the critical stress $\sigma_c$ the driving force curve and the R-curve are tangent. Beyond the point of tangency the driving force increases faster with crack length than does the material's resistance. This instability condition represents the failure of the body. The point of tangency defines the fracture toughness $G_c$ and the critical crack length $2a_c$. Since the driving force curve for an infinite body is a straight line, it should be apparent that both the fracture toughness $G_c$ and the amount of crack extension at instability $\Delta_c$ increase with increasing original crack length $2a_o$. If the R-curve exhibits a plateau, $G_c$ and $\Delta_c$ may asymptotically approach limit values.

In simple finite bodies and test specimens, the presence of stress-free boundaries results in an additional increase in the crack driving force as the crack extends toward a boundary. Thus the slope of the driving force curve increases continuously with increasing crack length. The instability condition for a typical finite-width specimen is shown in figure 2 and is determined as follows. For a given specimen configuration and loading, the dimensionless stress intensity calibration factor is defined as

$$Y \equiv \frac{K_I}{\sigma\sqrt{a}} = \text{fcn}(\lambda)$$

where $K_I$ is the opening-mode elastic stress intensity factor, $\lambda = na/W$ is the relative crack length, and $n$ is the number of crack tips (one or two). If we define a dimensionless sensitivity factor as

$$\alpha \equiv \frac{\lambda}{Y}\frac{dY}{d\lambda} \tag{1}$$

then (for constant stress) the crack driving force curve and its slope are

$$E'G_A = Y^2\sigma^2 a$$

$$E'\frac{dG_A}{da} = Y^2\sigma^2(1 + 2\alpha)$$

For convenience, the crack extension resistance curve and its slope are written here as

$$g(\Delta) \equiv E'G_R$$

$$g'(\Delta) \equiv E' \frac{dG_R}{d\Delta}$$

At the instability point, $G_A = G_R$ and $dG_A/da = dG_R/d\Delta$ (see fig. 2). If $g(\Delta)$ and $g'(\Delta)$ are mathematically describable, the instability point is determined by the simultaneous solution of the following equations:

$$E'G_c = Y_c^2 \sigma_c^2 (a_o + \Delta_c) = g(\Delta_c) \tag{2}$$

$$E' \left.\frac{dG}{da}\right|_{a_c} = Y_c^2 \sigma_c^2 (1 + 2\alpha_c) = g'(\Delta_c) \tag{3}$$

The coefficients $Y$ and $\alpha$ are usually expressed as trigonometric or polynomial functions of the relative crack length $\lambda$. As a result, a closed-form simultaneous solution is seldom possible, and numerical methods must be used to solve for $\Delta_c$. This can be done as follows. Dividing equation (2) by equation (3) and rearranging terms give

$$0 = \frac{g(\Delta_c)}{g'(\Delta_c)} - \frac{a_o + \Delta_c}{1 + 2\alpha_c} \tag{4}$$

If the functions $g(\Delta)$ and $g'(\Delta)$ and the appropriate equation for $\alpha$ are substituted into equation (4) then, for prescribed values of $a_o$ and $W$, $\Delta_c$ is the least positive root of equation (4). This root can be found by any of several numerical methods. Next, the function $g(\Delta)$ is evaluated at $\Delta_c$ to calculate $g(\Delta_c)$. Finally, the fracture stress $\sigma_c$ is obtained from equation (2) using the appropriate value of $Y_c$. In this report the expressions

$$Y = \left(\pi \text{ secant } \frac{\pi\lambda}{2}\right)^{1/2}$$

for the center-crack specimen (ref. 7) and

$$Y = \lambda^{-1/2}(1 - \lambda)^{-3/2}(2 + \lambda)(0.866 + 4.64\,\lambda - 13.32\,\lambda^2 + 14.72\,\lambda^3 - 5.6\,\lambda^4)$$

for the compact (tension) specimen (ref. 8; $\lambda \geq 0.2$) are used except where noted.

For a crack in an infinite body, both $G_c$ and $\Delta_c$ increase with increasing initial crack length. In a finite body, as the initial crack length is increased from zero, $G_c$ and $\Delta_c$ increase at first. However, due to the fact that $dY/d\lambda$ continually increases with $\lambda$, both $G_c$ and $\Delta_c$ reach maximum values which depend on the specimen width

W and the forms of both the driving force curve and the R-curve. As the initial crack length is increased still further, both $G_c$ and $\Delta_c$ begin to decrease. This behavior is shown schematically in figure 3 where instability curves are shown for a wide range of initial crack lengths. The locus of all instability points is shown by the dashed line. From figure 3 it is also apparent that there are pairs of initial crack lengths, say $(na_o)_1 = 0.2W$ and $(na_o)_2 \approx 0.7W$, which will have the same critical crack extension, $(\Delta_c)_{1,2}$, and fracture toughness, $(G_c)_{1,2}$. From equation (2), the fracture stresses for these initial crack lengths are related by

$$\frac{(\sigma_c)_2}{(\sigma_c)_1} = \frac{(Y_c)_1}{(Y_c)_2} \sqrt{\frac{(a_o)_1 + (\Delta_c)_{1,2}}{(a_o)_2 + (\Delta_c)_{1,2}}}$$

Thus there is a relation between fracture stresses for short cracks and long cracks which is implicit in the R-curve concept, and this relation is a function of the specimen type and the shape of the R-curve.

If an equation for the R-curve is available, residual strength can be calculated for any specimen size and configuration using the procedure which follows equation (4). If the R-curve equation has a simple form, it is sometimes possible to develop a dimensionless residual strength curve. For example, suppose the R-curve is given by

$$g(\Delta) = A\Delta^b$$

where $b < 1.0$. Then for center-crack specimens the residual strengths are as shown in figure 4 for two values of the exponent, $b = 0.5$ (a parabola) and $b = 0.2$. For this case the shape of the residual strength curve depends only on the exponent b. Here it is obvious that the R-curve concept implies a particular residual strength curve which is a function of the specimen type and the R-curve shape. This implication will be useful in later comparisons of R-curves and semiempirical analyses.

In concluding this section it should be emphasized that, in this report, $\Delta$ is the effective crack extension. It is the sum of the physical crack extension plus an adjustment to account for the effect of crack tip plasticity. The nature of the plasticity adjustment, although technically significant, has no influence on the analyses and conclusions in this report.

## EQUIVALENCY ANALYSIS

In the preceding section it was shown that, if a mathematical formulation of the R-curve is available, fracture stress can be determined as a function of original crack

length. In this section it will be shown that, if an equation for fracture stress as a function of original crack length is available, the equivalent R-curve can be determined.

To do this we must differentiate equation (2) with respect to $\Delta_c$, and that operation requires some prior consideration. For a given specimen type, there are many combinations of specimen width and initial crack length which will result in instability at the same point on the R-curve, and each combination has an associated fracture stress. To cause a small change ($d\Delta_c$) in the instability point, there must be a change in the specimen width or the initial crack length or both, and there will be a change in the fracture stress. Thus, when differentiating equation (2), the terms W, $\sigma$, and $a_o$ are treated as variables. First, note that

$$\frac{dY}{d\Delta} = \frac{\partial Y}{\partial a_o}\frac{da_o}{d\Delta} + \frac{\partial Y}{\partial \Delta}\frac{d\Delta}{d\Delta} + \frac{\partial Y}{\partial W}\frac{dW}{d\Delta} = \frac{n}{W}\frac{dY}{d\lambda}\left(\frac{da_o}{d\Delta} + 1 - \frac{a_o + \Delta_c}{W}\frac{dW}{d\Delta}\right)$$

Now, differentiating both sides of equation (2) with respect to $\Delta_c$ yields

$$\frac{d}{d\Delta_c}E'G_c = Y_c^2\sigma_c^2 2\alpha_c\left(\frac{da_o}{d\Delta_c} + 1 - \frac{a_o + \Delta_c}{W}\frac{dW}{d\Delta_c}\right) + Y_c^2(a_o + \Delta_c)\frac{d}{d\Delta_c}\left(\sigma_c^2\right)$$

$$+ Y_c^2\sigma_c^2\left(\frac{da_o}{d\Delta_c} + 1\right) \equiv g'(\Delta_c)$$

and substituting equation (3) results in

$$0 = \sigma_c^2\left[(1 + 2\alpha_c)\frac{da_o}{d\Delta_c} - 2\alpha_c\frac{a_o + \Delta_c}{W}\frac{dW}{d\Delta_c}\right] + (a_o + \Delta_c)\frac{d}{d\Delta_c}\left(\sigma_c^2\right) \qquad (5)$$

At this point it is helpful to reduce the problem to one of a single independent variable by prescribing the manner in which $a_o$ and W may vary. Three cases will be considered.

Case I: W = Constant (dW = 0)

Assume that there is a function f such that we can define

$$\left.\begin{aligned} f(a_o) &\equiv \sigma_c^2 \\ f'(a_o) &\equiv \frac{d\left(\sigma_c^2\right)}{da_o} \end{aligned}\right\} \text{for } W = \text{constant}$$

Then equation (5) becomes

$$0 = \frac{da_o}{d\Delta_c}\left[(1 + 2\alpha_c)f(a_o) + (a_o + \Delta_c)f'(a_o)\right]$$

and, since $da_o/d\Delta_c \neq 0$, we have

$$0 = (1 + 2\alpha_c)f(a_o) + (a_o + \Delta_c)f'(a_o) \tag{6a}$$

Case II: $a_o/W = \text{Constant}$ $\left[dW = (W/a_o)da_o\right]$

Now assume that there is a function $h$ such that

$$\left.\begin{aligned} h(a_o) &\equiv \sigma_c^2 \\ h'(a_o) &\equiv \frac{d\left(\sigma_c^2\right)}{da_o} \end{aligned}\right\} \text{for } \frac{a_o}{W} = \text{constant}$$

Now equation (5) becomes

$$0 = \frac{da_o}{d\Delta_c}\left[\left(1 - 2\alpha_c \frac{\Delta_c}{a_o}\right)h(a_o) + (a_o + \Delta_c)h'(a_o)\right]$$

and since $da_o/d\Delta_c \neq 0$, we have

$$0 = \left[\left(1 - 2\alpha_c \frac{\Delta_c}{a_o}\right)h(a_o) + (a_o + \Delta_c)h'(a_o)\right] \tag{6b}$$

Case III: $a_o$ = Constant ($da_o = 0$)

This case is of limited usefulness but is included for completeness. Assume that there is a function j such that

$$\left.\begin{aligned} j(W) &\equiv \sigma_c^2 \\ j'(W) &\equiv \frac{d\left(\sigma_c^2\right)}{dW} \end{aligned}\right\} \text{for } a_o = \text{constant}$$

Now equation (5) becomes

$$0 = \frac{dW}{d\Delta_c}(a_o + \Delta_c)\left[-\frac{2\alpha_c}{W} j(W) + j'(W)\right]$$

and since $dW/d\Delta_c \neq 0$ and $(a_o + \Delta_c) \neq 0$,

$$0 = -\frac{2\alpha_c}{W} j(W) + j'(W) \tag{6c}$$

For cracks in infinite bodies, $\alpha = 0$ and equation (6a) becomes

$$\Delta_c = \frac{f(a_o)}{-f'(a_o)} - a_o \tag{7}$$

which, after substituting the infinite-body formulations for $f(a_o)$ and $f'(a_o)$ from the Appendix, gives $\Delta_c$ for any $a_o$ in terms of the empirical parameters. Then terms can be rearranged to give $a_o$ as a function of $\Delta_c$, say

$$a_o = F(\Delta_c)$$

Substituting this function into equation (2) yields

$$E'G_c = Y_c^2\left[F(\Delta_c) + \Delta_c\right] \cdot f\left[F(\Delta_c)\right] \tag{8a}$$

Since equation (7) gives $\Delta_c$ for any value of $a_o$, equation (8a) must give $E'G_c$ for any and all values of $\Delta_c$, which is a definition of the R-curve. Thus, after writing the function F in terms of the empirical parameters, it is appropriate to write equation (8a) in the general terms of $E'G_R$ and $\Delta$, rather than $E'G_c$ and $\Delta_c$. The end result is an explicit ERC formulation in terms of the empirical parameters.

To determine the ERC for cracks in finite bodies, an indirect method is required. First, the finite-body formulation for f, h, or j and its derivative (see the Appendix) are substituted into the appropriate one of equations (6). Because of the more complicated nature of the finite-body formulations, it is unlikely that an explicit function $F(\Delta_c)$ will be obtainable. But for any given value of $\Delta_c$, $a_o$ is a root of equation (6) which may be found by standard numerical methods and which represents a single value of $F(\Delta_c)$. For Case III, of course, one determines $W = F(\Delta_c)$ and solves for $W$ as a root of equation (6c). Substituting the root into equation (8a) (if Case I) or into

$$E'G_c = Y_c^2\left[F(\Delta_c) + \Delta_c\right] \cdot h\left[F(\Delta_c)\right] \qquad \text{if Case II} \qquad (8b)$$

$$E'G_c = Y_c^2\left[F(\Delta_c) + \Delta_c\right] \cdot j\left[F(\Delta_c)\right] \qquad \text{if Case III} \qquad (8c)$$

as appropriate yields a discrete point on the ERC. By incrementing $\Delta_c$ and repeating the calculation, the ERC can be determined point by point.

## ANALYTICAL COMPARISONS

### Dimensionless Equivalent R-Curves

It is helpful and more efficient to first compare semiempirical fracture analyses (SEFA) and equivalent R-curves (ERC) on an analytical basis. This is most easily done using the problem of a crack in an infinite plate as a baseline.

The infinite-body ERC for Kuhn's analysis (ref. 1) is obtained using the method described in the paragraph containing equations (7) and (8a). Substituting equations (A1) and (A2) from the Appendix into equations (7) and (8a) with $Y_c^2 = \pi$ yields

$$\Delta_c = \frac{\sqrt{a_o}}{C_m} \qquad (9a)$$

$$E'G_R = \frac{\pi\sigma_u^2 \Delta}{1 + C_m^2 \Delta} \qquad (10a)$$

where $C_m$ is an empirical parameter having units $(L^{-1/2})$. Equation (10a) is plotted in dimensionless form in figure 5(a). This curve obviously resembles an R-curve and might be expected to closely match some (but not all) experimental R-curves.

The infinite-body ERC for Orange's analysis (ref. 2) is obtained in the same manner. Using equations (A3) and (A4) results in

$$\Delta_c = \frac{\left(\frac{K_u}{\sigma_u}\right)^2}{\pi} \tag{9b}$$

$$E'G_R = K_u^2 \tag{10b}$$

where $K_u$ is an empirical parameter having units $(FL^{-3/2})$. These equations define a single point. In order to relate this single point to the R-curve concept, the point may be thought of as the corner of a step-function, and that step-function might in turn be considered as a very simple approximation of an actual R-curve.

The infinite-body ERC for Feddersen's analysis (ref. 3) is obtained by substituting equations (A5) and (A6) into equations (7) and (8a) as before, yielding

$$\Delta_c = \frac{27}{8\pi}\left(\frac{K_c}{\sigma_{ys}}\right)^2 - \frac{3}{2}a_o \tag{9c}$$

$$E'G_R = K_c^2\left\{1 + \left[\frac{4\pi}{9}\left(\frac{\sigma_{ys}}{K_c}\right)^2\Delta\right] + \frac{1}{3}\left[\frac{4\pi}{9}\left(\frac{\sigma_{ys}}{K_c}\right)^2\Delta\right]^2 + \frac{1}{27}\left[\frac{4\pi}{9}\left(\frac{\sigma_{ys}}{K_c}\right)^2\Delta\right]^3\right\} \tag{10c}$$

for $a_o \leq (9/4\pi)(K_c/\sigma_{ys})^2$ where $K_c$ is an empirical parameter having units $(FL^{-3/2})$. Equation (9c) requires that critical crack extension decrease as original crack length increases from zero. This is in direct opposition to the R-curve concept and is not supported by any data known to this author. Equation (10c), which is plotted in figure 5(b), does not look at all like an R-curve but does satisfy the requirements of coincidence and tangency. For $a_o = 0$, the point of tangency is the right terminus of the curve. As $a_o$ increases, the point of tangency moves downward and leftward along the curve. Finally, at $a_o = (9/4\pi)(K_c/\sigma_{ys})^2$, the point of tangency is the left terminus.

The infinite-body ERC for Newman's analysis (ref. 4) is obtained by substituting equations (A11) and (A12) into equations (7) and (8a) as before, yielding

$$\Delta_c = \frac{mK_f}{\sigma_u}\sqrt{\frac{a_o}{\pi}} \tag{9d}$$

$$E'G_R = \frac{\sigma_u^2 \Delta}{\frac{m^2}{\pi} + \left(\frac{\sigma_u}{K_f}\right)^2 \Delta} \tag{10d}$$

where $K_f$ is an empirical parameter having units $(FL^{-3/2})$ and $m$ is a dimensionless empirical coefficient which is not greater than unity. Equation (10d) is plotted in dimensionless form in figure 5(c). This ERC is asymptotic to $E'G_R = K_f^2$, and the coefficient $m$ determines the rapidity of the approach. As $m$ decreases from unity to near-zero, the ERC develops a progressively sharper knee. The flexibility of this two-parameter ERC should allow it to match R-curves for a wide range of real materials.

The infinite-body ERC for Bockrath's analysis (ref. 5) is obtained by substituting equations (A15) and (A16) into equations (7) and (8a) as before, resulting in

$$\Delta_c = \left(\frac{\omega}{2}\right) a_o \tag{9e}$$

$$E'G_R = \frac{\pi}{2}(2 + \omega) K_{Tc}^2 \left(\frac{2}{\omega} \Delta\right)^{\omega/(2+\omega)} \tag{10e}$$

where $\omega$ is a dimensionless empirical coefficient and $K_{Tc}$ is an empirical parameter having irrational units $(FL^{\omega})$. Equation (10e) is plotted in figure 5(d). This ERC has no asymptote, and its slope is infinite at $\Delta = 0$. Except for notation, it is identical to the R-curve model proposed by Broek as equation (10) of reference 9. Broek's model was derived using R-curve concepts and the experimental observation that, for small cracks in wide specimens, the critical crack length is often proportional to the initial crack length.

At this point we can state the following. For each SEFA, in its infinite-body form at least, there is indeed an ERC. For four of the analyses considered, the ERC resembles or approximates an actual R-curve. The ERC for Feddersen's analysis does not resemble an R-curve and will not be considered further.

## Comparisons Using Synthetic Data

Hypothesis (2) of the INTRODUCTION postulates that a SEFA will correlate residual strength data closely if its ERC closely matches the actual R-curve and will correlate poorly if the match is poor. To test this hypothesis we would need, as a minimum, both residual strength data (over a wide range of crack lengths) and R-curve data for two

materials having significantly different R-curve shapes. Further, it would be desirable to have data for several specimen sizes (including quasi-infinite) and specimen types. Since no such body of data is known to this author, it was necessary to synthesize one. This was done by formulating two R-curve equations using the following guidelines. First, to avoid exact fits, neither equation should be mathematically equivalent to one of of the ERC formulations previously derived. Second, one curve should have a definite knee, the other should be gently curving. Using these two R-curve equations, synthetic test data can be calculated by instability analysis for any specimen size and type. A practical advantage of this approach is the total absence of data scatter.

Unobtainium is assumed to be a heat-treatable material. In the annealed condition, its ultimate tensile strength is 150 and its R-curve is given by

$$E'G_R = 8000 \sqrt{10\,\Delta - \Delta^2} \tag{11a}$$

Since the material is imaginary, the units will be left to the reader's imagination. In the aged condition, its ultimate tensile strength is 200 and its R-curve is given by

$$E'G_R = \frac{50\,000}{\pi} \arctan\,(10\,\Delta) \tag{11b}$$

These are shown in figure 6. The coefficients in equations (11) were selected so that the significant features of both curves would lie within the ranges $0 \le E'G_R \le 25\,000$ and $0 \le \Delta \le 1$.

The pseudotest data points are calculated using conventional instability analysis as described in the paragraph containing equation (4). The "specimens" that are studied here were sized as follows. For the infinite-width pseudotests, the initial crack half-lengths $a_o$ were chosen (by trial and error) to give $\Delta_c$ values well distributed over the entire R-curve. For the finite-width center-crack pseudotests, the same initial crack lengths were used but the specimen widths were fixed at eight times (first series) and four times (second series) the largest initial crack half-length. For the compact specimens, the ratio $a_o/W$ was fixed at 0.5 and the widths chosen (again by trial and error) to give approximately the same $\Delta_c$ values as those calculated for the infinite-width pseudotests. The calculated values of stress and crack extension at instability are given in table I. The values of stress and initial crack length were then used as inputs to the various semiempirical analyses.

The empirical parameters were determined as follows. Kuhn's parameter $C_m$ was calculated for each specimen in the infinite-width series using equation (A1). The simple average of seven values $\overline{C}_m$ is given in table I. The bar is used here to denote the average value for one data set. Orange's parameter $K_u$ was also calculated for

each specimen in the infinite-width series using equation (A3). The average value $\overline{K}_u$ given in table I is a weighted average determined in the same manner as equation (6) of reference 2. Newman's parameters $\overline{K}_f$ and $\overline{m}$ were determined using the least-squares procedure given in Appendix C of reference 4. Bockrath's parameters $\overline{K}_{Tc}$ and $\overline{\omega}$ were determined by a least-squares fit of equation (A15). Since Bockrath's method is restricted to cases where the crack area is less than 10 percent of the gross area, specimens having $a_o > W/20$ were excluded from the fit.

The equivalent R-curves were calculated as follows. For the infinite-width series, the empirical parameters from table I were simply substituted into the appropriate one of equations (10). For the remaining series, the indirect method (described in the paragraph containing eqs. (8b) and (8c)) was used. Specifically, for the finite-width center-crack series, equations (A9) and (A10) or equations (A15) and (A16) were used along with equations (6a) and (8a) and the appropriate empirical parameters. For the compact specimen series, equations (A13), (A14), (6b), and (8b) were used.

When determining the Newman ERC for constant-finite-width specimen configurations, some precautions must be taken. For values of $\Delta_c$ near zero, there are three positive roots of equation (6a); one at $\lambda_o$ near zero, one at $\lambda_o \sim 0.44$, and one at $\lambda_o$ near unity. The middle root gives an ERC which resembles the Feddersen ERC of figure 5(b) and which should be ignored. The other two roots give ERCs which are numerically similar but distinctly different. As discussed earlier in the section R-CURVE CONCEPTS, the R-curve concept implies a particular relation between fracture stresses for short cracks and long cracks. Since Newman's analysis does not match this relation, we have separate ERCs for short and long cracks. As the value of $\Delta_c$ is increased, the middle root converges upon one of the other roots whereupon the converged roots vanish. In this report, the Newman ERC for constant-finite-width configurations is determined using the least positive root of equation (6a) over the range of $\Delta_c/W$ for which three positive roots exist.

The residual strength of the infinite-width Unobtainium is shown in figure 7. For the annealed condition, Bockrath's semiempirical fracture analysis (SEFA) provides a nearly perfect fit to the pseudodata. When ranked according to the sum of the squares of the deviations, Newman's SEFA, Kuhn's, and Orange's follow in that order. For the aged condition, the ranking is quite different. Here Newman's SEFA provides a nearly perfect fit, with Orange's, Kuhn's, and Bockrath's following in that order. The equivalent R-curves (ERCs) are shown in figure 8. For the annealed condition, the Bockrath ERC matches the actual R-curve almost perfectly. When ranked according to the integral of the square of the deviation, the Newman ERC, the Kuhn ERC, and the Orange ERC follow in that order. For the aged condition, the Newman ERC is the best match to the actual R-curve. The Kuhn ERC, the Bockrath ERC, and the Orange ERC follow

in that order. The Orange ERC, although crude, is a better match to the aged material than to the annealed.

Critical crack extensions derived from the Newman and Bockrath ERCs are shown in figure 9. The Bockrath ERC predicts crack extension fairly closely for the annealed condition, but neither ERC gives a very good prediction for the aged condition. This last observation should not be surprising. Returning to figure 2, it should be apparent that a small change in the slope of the R-curve near the instability point will cause a large change in the critical crack extension but only a small change in the critical stress. Thus when instability calculations are made from any R-curve, be it actual or equivalent, fracture stress can be predicted with much more confidence than can crack extension.

Since the Orange ERC is rather crude and since Kuhn's SEFA is equivalent to a special case of Newman's (see the Appendix, following eq. (A12)), these two were not considered further. The Newman and Bockrath ERCs for the finite-width center-crack series are shown in figures 10 and 11. Here the same trends are seen as in the infinite-width series. The Bockrath ERC is the better match for the annealed condition, while the Newman ERC is the better match for the aged condition. Note in table I that the empirical parameters $\overline{K}_{Tc}$, $\overline{\omega}$, $\overline{K}_f$, and $\overline{m}$ all vary slightly with specimen width. The ERCs shown in figures 8, 10, and 11 are also distinctly different for different specimen widths, but the differences are slight.

Since Bockrath's SEFA does not include the compact specimen geometry, only the Newman ERC was determined for the compact specimen series. Note again in table I that Newman's empirical parameters for the compact specimen series differ from those obtained for the various center-crack series. The differences in the parameter $\overline{K}_f$ are slight; the differences in $\overline{m}$ are somewhat larger. The Newman ERCs for the compact specimen series are shown in figure 12. The correspondence between equivalent and actual R-curves is not quite as close as for the center-crack series, but the general trend is the same. A much better match is obtained for the aged condition than for the annealed.

The results of this exercise using synthetic data can be summarized as follows. Hypothesis (2) of the INTRODUCTION postulates that an SEFA will correlate residual strength data closely if its ERC closely matches the actual R-curve and will correlate poorly if the match is poor. Strictly speaking, this hypothesis cannot be proven, since the ERC magnitude and shape depend on empirical parameters which must be obtained from residual strength data. However, the converse appears to be true. That is, if an SEFA correlates residual strength data closely, its ERC will closely match the actual R-curve. Furthermore, it is apparent that if, for a given material and thickness, the R-curve is unique the various empirical parameters are not, and vice versa. Also, although it is possible to predict the critical crack length in terms of the original crack

length and the empirical parameters, this cannot be recommended. The crack extension at instability is quite sensitive to small differences in the slope and magnitude of the R-curve near the instability point.

## COMPARISONS USING ACTUAL TEST DATA

As mentioned earlier, experimental studies containing both residual strength and actual R-curve data are relatively few in number. Nevertheless, enough were found in the literature to allow some comparisons to be made using actual data obtained from real materials.

### NASA Data for 2014-T6 Aluminum Alloy

In reference 10 this author presented test data for 2014-T6 aluminum alloy specimens 1.5 millimeters (0.06 in.) thick, tested at 77 K (-320° F). Figure 14 in reference 10 presented typical curves of crack growth against applied stress for notches of six initial lengths in 30-centimeter (12-in.) wide specimens. Those curves were developed by plotting individual crack growth data points for replicate specimens, then drawing a smooth curve to give a good visual average. For the present report, those data were reanalyzed. The crack extension resistance and effective crack length were computed for each data point as

$$E'G_R = \sigma^2 \pi a_{eff} \text{ secant} \left( \frac{\pi a_{eff}}{W} \right)$$

$$a_{eff} = a + \left( \frac{E'G_R}{2\pi\sigma_{ys}^2} \right)$$

respectively. Since these equations are transcendental, an iterative solution was required. A total of 176 data points were obtained from 17 specimens with initial crack lengths $2a_o$ ranging from 3 to 100 millimeters (1/8 to 4 in.). The empirical parameters for the Newman and Bockrath SEFAs were determined in the manner described earlier. As before, only specimens with $a_o \leq W/20$ were included in the Bockrath analysis. The fitted empirical parameters are listed in table II.

Residual strength is shown in figure 13. Newman's SEFA gives a good fit over the entire range. Bockrath's SEFA fits the short-crack data fairly well, but the fit would be poor if extrapolated to longer cracks. The R-curve data points and the equivalent

R-curves are shown in figure 14. Both ERCs fit the data rather well, with Bockrath's somewhat better at small crack extensions and Newman's somewhat better for larger extensions. These results suggest that the ERC concept applies to real data as well as to synthesized data.

## Battelle Data for 7075-T7351 Aluminum Alloy

Reference 11 contains test data for 7075-T7351 aluminum alloy specimens 25 millimeters (1.0 in.) thick and 40 centimeters (16 in.) wide. This data set is unusual in that the ratios of initial crack length to plate width range uniformly from near-zero to near-unity; also, the specimens were instrumented to measure crack opening displacement (COD) during loading, and the stress corresponding to a 5-percent secant offset on the load-COD curve is reported. A secant offset corresponds to an increase in the effective crack length. From an R-curve one should be able to predict the stress required to cause such an increase.

Since Bockrath's analysis is restricted to small cracks, only the Newman ERC was used here. First Newman's empirical parameters were determined by fitting the residual strength data as described earlier. The stress at 5 percent secant offset is calculated as follows. According to reference 12, the crack opening displacement $\delta$ for a finite-width center-crack plate is

$$\delta = \left(\frac{4\sigma a}{E'}\right) V_1(\lambda)$$

where

$$V_1(\lambda) = -0.071 - 0.535\,\lambda + 0.169\,\lambda^2 + 0.020\,\lambda^3 - 1.071\,\lambda^{-1}\ln(1-\lambda)$$

The slope of the load-COD curve is thus proportional to

$$\frac{4\sigma}{E'\delta} = \left[aV_1(\lambda)\right]^{-1}$$

Let $\Delta_5$ be the crack extension at 5 percent secant offset. Then a crack of half-length $a_o + \Delta_5$ will give a slope 5 percent less than a crack of half-length $a_o$, or

$$\left[(a_o + \Delta_5)V_1(\lambda_5)\right]^{-1} = 0.95\left[a_o V_1(\lambda_o)\right]^{-1}$$

where $\lambda_5 = 2(a_o + \Delta_5)/W$. Rearranging terms results in

$$0 = \frac{1}{0.95} \frac{V_1(\lambda_o)}{V_1(\lambda_5)} - \frac{a_o + \Delta_5}{a_o}$$

and $\Delta_5$ is the least positive root of the previous equation, which may be found by standard numerical methods. Now that $\Delta_5$ is known, the corresponding crack extension resistance $E'G_5$ is obtained from the Newman ERC. Finally the stress at 5 percent secant offset $\sigma_5$ is

$$\sigma_5 = \frac{\sqrt{E'G_5/\pi(a_o + \Delta_5) \text{ secant } \pi(a_o + \Delta_5)/W}}{1 - 0.025\,\lambda_5^2 + 0.06\,\lambda_5^4} \tag{12}$$

Here the modified-secant stress intensity factor expression from reference 12 was used for greater accuracy at relative crack lengths near unity.

The fitted empirical parameters are given in table II. Residual strength is shown in figure 15, where Newman's SEFA can be seen to fit the data reasonably well. The stress at 5 percent secant offset is shown in figure 16. Except for the shortest crack, the stress predicted by equation (12) agrees well with the reported data, the scatter being no worse than the scatter in the residual strength. Since the length of the shortest crack is less than twice the plate thickness, it is likely that the two-dimensional representation implicit in the analyses is no longer valid. The otherwise good agreement suggests that, even though the actual R-curve is not available for comparison, the Newman ERC must closely approximate it.

## Alcoa Data for Compact Specimens

Reference 13 contains test data for compact specimens of 2219-T851 aluminum alloy in four thicknesses. Specimen sizes were varied, but the initial crack length was always half the specimen width. The maximum loads and the loads designated $P_Q$ are reported. The load $P_Q$ is the load corresponding to a 5-percent secant offset on the load-COD curve and is used to compute the plane strain fracture toughness $K_{Ic}$. As was done for the Battelle center-crack specimens, one should be able to predict these loads from an ERC.

Since Bockrath's SEFA has not been formulated for the compact specimen geometry, only Newman's SEFA is examined here. Newman's empirical parameters were determined for each thickness in the manner described earlier for compact specimens.

According to reference 14, the crack opening displacement $V_o$ measured in a $K_{Ic}$ test is given by

$$\frac{2E'V_o}{P} = 120.7 - 1065.3\,\lambda + 4098.2\,\lambda^2 - 6688.0\,\lambda^3 + 4450.5\,\lambda^4$$

Using this expression, the crack extension corresponding to a 5-percent secant offset with $a_c/W = 0.5$ is $\Delta_5 = 0.023\,a_o$ and the corresponding crack extension resistance $E'G_5$ is thus obtainable from the Newman ERC for the appropriate thickness. The load $P_Q$ is then

$$P_Q = \frac{BW}{Y_5}\sqrt{\frac{E'G_5}{a_o + \Delta_5}} \tag{13}$$

where B is the specimen thickness and $Y_5$ is the stress intensity calibration factor corresponding to $a = a_o + \Delta_5 = 1.023\,a_o$. The equation from reference 8 given following equation (4) in this report gives $Y_5 = 13.79$ for $\lambda = 0.5115$.

The predicted loads $P_Q$ for each thickness are shown in figure 17. Agreement with the reported test loads is generally good, with the average error for the 32 tests being about 8 percent and the largest absolute error being less than 9 KN (2 kip). This figure indicates that the Newman ERC can also approximate the actual R-curve using residual strength data from compact specimens.

## Boeing Data for 2219-T87 Aluminum Alloy

Earlier it was shown using synthetic data that, if the actual R-curve is unique, one obtains slightly different values of the empirical parameters from data sets for specimens having different widths. Data from the Boeing Co. for 2219-T87 aluminum alloy specimens have the same characteristics. These data originally appeared in an internal report (Eichenberger, T. W.: Fracture Resistance Data Summary. Report D2-20947, Boeing Airplane Co., June 1962) but are also tabulated in reference 1. Center-crack specimens 2.5 millimeters (0.10 in.) thick were tested. The data for specimens 60 and 120 centimeters (24 and 48 in.) wide are used here because they cover a wide range of crack lengths.

Bockrath's analysis was not applied since only one of the wider specimens had $a_o \leq W/20$. Newman's parameters were determined separately for each specimen width, and somewhat different values were obtained as can be seen in table II. The residual strength curves fit the data quite well, as can be seen in figure 18, with the average

error being less than $3\frac{1}{2}$ percent. Using a method that is outside the scope of this report, it was found that the actual R-curve for this material could be estimated by

$$E'G_R = 8.07\times10^{15}\ \Delta^{0.554}$$

where $E'G_R$ is in $N^2/m^3$ and $\Delta$ is in cm, or by

$$E'G_R = 11.2\times10^{9}\ \Delta^{0.554}$$

where $E'G_R$ is in $lb^2/in.^3$ and $\Delta$ is in inches. Residual strengths calculated from this equation using conventional instability analysis are also shown in figure 18. The agreement is very slightly better than for Newman's SEFA, the average error being less than 3 percent. The estimated R-curve and the Newman ERCs are shown in figure 19, and as expected the differences are small. Although these data tend to support the concept of a unique R-curve, the differences are so small as to be within the bounds of probable data scatter.

## CONCLUDING REMARKS

The relations between several semiempirical fracture analyses (SEFA) and the R-curve concept of fracture mechanics are examined and the conditions for equivalence between a SEFA and an R-curve are derived. A hypothetical material is employed to study the relation analytically. Equivalent R-curves are developed for several real materials using data from the literature. The results of this study lead to the following conclusions:

1. For each semiempirical fracture analysis (SEFA) there is an equivalent R-curve (ERC) whose magnitude and shape are determined by the SEFA formulation and its empirical parameters. The ERC is equivalent in that it predicts exactly the same relation between fracture stress and initial crack length (residual strength) as the SEFA.

2. If, for a given set of data, a SEFA correlates residual strength closely, its ERC will closely approximate the effective R-curve of the material.

3. It is possible to predict the critical crack length in terms of the initial crack length and the fitted empirical parameters. However, this is not recommended since the crack extension at instability is particularly sensitive to the slope of the R-curve.

4. Of the five SEFAs examined, Newman's appears to be the most generally useful. Bockrath's SEFA, which is only formulated for quasi-infinite bodies, is too restrictive for widespread use. Three other SEFAs do not appear to warrant further consideration.

5. If the effective R-curve is unique, then the various empirical parameters cannot be constant, and vice versa.

The analytical comparisons made herein indicate that the variations in Newman's parameters are small enough that the differences may well be within the range of normal data scatter for real materials. Thus a very carefully planned and conducted experiment would be required to determine which concept (R-curve or SEFA) is more universally applicable.

Lewis Research Center,
National Aeronautics and Space Administration,
Cleveland, Ohio, September 18, 1979,
505-02.

## APPENDIX - SEMIEMPIRICAL FRACTURE ANALYSES

In this Appendix, equations from references 1 to 5 are rewritten using the notation of this report. Note the following definitions from the text:

$$\left.\begin{aligned} f(a_o) &\equiv \sigma_c^2 \\ f'(a_o) &\equiv \frac{d\left(\sigma_c^2\right)}{da_o} \end{aligned}\right\} \text{for } W = \text{constant}$$

$$\left.\begin{aligned} h(a_o) &\equiv \sigma_c^2 \\ h'(a_o) &\equiv \frac{d\left(\sigma_c^2\right)}{da_o} \end{aligned}\right\} \text{for } \frac{a_o}{W} = \text{constant}$$

P. Kuhn (1968)

Equations (3) and (4) of reference 1 give the fracture stress for a finite-width center-crack plate as

$$\sigma_c = \sigma_u(1 - \lambda_o)\left[1 + C_m\sqrt{a_o(1 - \lambda_o)(1 + \lambda_o)}\right]^{-1}$$

where $C_m$ is an empirical parameter having units $(L^{-1/2})$. Thus for an infinite plate,

$$f(a_o) = \sigma_u^2\left(1 + C_m\sqrt{a_o}\right)^{-2} \tag{A1}$$

$$f'(a_o) = -f(a_o)\left(1 + C_m\sqrt{a_o}\right)^{-1}\frac{C_m}{\sqrt{a_o}} \tag{A2}$$

T. Orange (1969)

Equation (8) of reference 2 gives the fracture stress for a finite-width center-crack plate as

$$\sigma_c^2 = K_u^2 \Big/ W \tan\left[\frac{\pi a_c}{W} + \arctan\left(\frac{K_u^2}{\sigma_u^2 W}\right)\right]$$

where $K_u$ is an empirical fracture toughness parameter having units $(FL^{-3/2})$. For an infinite plate, this reduces to

$$f(a_o) = K_u^2\left[\pi a_o + \left(\frac{K_u}{\sigma_u}\right)^2\right]^{-1} \tag{A3}$$

$$f'(a_o) = -f(a_o)\left(a_o + \frac{K_u^2}{\pi\sigma_u^2}\right)^{-1} \tag{A4}$$

C. Feddersen (1970)

In reference 3, the fracture stress for a finite-width center-crack plate is given in equations (6) and (10) by

$$\sigma_c = \sigma_{ys}\left[1 - \frac{4\pi}{27}\left(\frac{\sigma_{ys}}{K_c}\right)^2 a_o\right] \qquad \text{for } a_o \le \frac{9}{4\pi}\left(\frac{K_c}{\sigma_{ys}}\right)^2$$

and in equation (7) by

$$\sigma_c = K_c(\pi a_o)^{-1/2} \qquad \text{for } \frac{9}{4\pi}\left(\frac{K_c}{\sigma_{ys}}\right)^2 \le a_o \le \frac{W}{6}$$

and in equations (8) and (11) by

$$\sigma_c = \frac{3}{2}(1 - \lambda_o)\sqrt{\frac{6K_c^2}{\pi W}} \qquad \text{for } a_o \geq \frac{W}{6}$$

where $\sigma_{ys}$ is the material's yield strength and $K_c$ is an empirical fracture toughness parameter. For an infinite plate, the first of these three equations reduces to

$$f(a_o) = \sigma_{ys}^2\left[1 - \frac{4\pi}{27}\left(\frac{\sigma_{ys}}{K_c}\right)^2 a_o\right]^2 \tag{A5}$$

$$f'(a_o) = -f(a_o)\left[\frac{27}{8\pi}\left(\frac{K_c}{\sigma_{ys}}\right)^2 - \frac{a_o}{2}\right]^{-1} \tag{A6}$$

and the second to

$$f(a_o) = K_c^2(\pi a_o)^{-1} \tag{A7}$$

$$f'(a_o) = \frac{-f(a_o)}{a_o} \tag{A8}$$

J. Newman (1972)

Equation (12) of reference 4 gives the fracture stress for a finite-width center-crack plate as

$$\sigma_c = K_f\left[\sqrt{\pi a_o \sec\left(\frac{\pi a_o}{W}\right)} + \frac{m}{1 - \lambda_o}\frac{K_f}{\sigma_u}\right]^{-1}$$

where $K_f$ is an empirical fracture toughness parameter and $m$ is a dimensionless empirical coefficient which is not greater than unity. Rewritten and differentiated, this is

$$f(a_o) = K_f^2 \left[ \sqrt{\pi a_o \sec\left(\frac{\pi a_o}{W}\right)} + \frac{1}{1 - \lambda_o} \frac{mK_f}{\sigma_u} \right]^{-2} \tag{A9}$$

$$f'(a_o) = -\frac{f(a_o)}{a_o} \frac{\left[1 + \frac{\pi a_o}{W} \tan\left(\frac{\pi a_o}{W}\right)\right] \sqrt{\pi a_o \sec\left(\frac{\pi a_o}{W}\right)} + \frac{2\lambda_o}{(1 - \lambda_o)^2} \frac{mK_f}{\sigma_u}}{\sqrt{\pi a_o \sec\left(\frac{\pi a_o}{W}\right)} + \frac{1}{1 - \lambda_o} \frac{mK_f}{\sigma_u}} \tag{A10}$$

which, for an infinite plate, reduce to

$$f(a_o) = K_f^2 \left( \sqrt{\pi a_o} + \frac{mK_f}{\sigma_u} \right)^{-2} \tag{A11}$$

$$f'(a_o) = -f(a_o) \sqrt{\frac{\pi}{a_o}} \left( \sqrt{\pi a_o} + \frac{mK_f}{\sigma_u} \right)^{-1} \tag{A12}$$

Note that, if we let $m = 1$ and $k_f = \sigma_u \sqrt{\pi}/C_m$, equation (A11) reduces to equation (A1). For the compact (tension) specimen, equations (1), (7), and (16) to (19) of reference 15 result in

$$h(a_o) = K_f^2 \left[ Y_o \sqrt{a_o} + \frac{1}{L(1 - \lambda_o)} \frac{mK_f}{\sigma_u} \right]^{-2} \tag{A13}$$

$$h'(a_o) = -h(a_o) \left[ Y_o \sqrt{a_o} + \frac{1}{L(1 - \lambda_o)} \frac{mK_f}{\sigma_u} \right]^{-1} \frac{Y_o}{\sqrt{a_o}} \tag{A14}$$

where

$$L = \sqrt{1 + \left(\frac{1 + \lambda_o}{1 - \lambda_o}\right)^2} - \left(\frac{1 + \lambda_o}{1 - \lambda_o}\right)$$

G. Bockrath (1972)

Equation (13) of reference 5 gives the fracture stress for a center-crack plate as

$$\sigma_c = K_{Tc}(a_o)^{-1/(2+\omega)}$$

where $\omega$ is a dimensionless empirical coefficient and $K_{Tc}$ is an empirical toughness parameter having irrational units of $(FL^{\omega})$. This equation is limited to $\lambda_o \leq 0.1$, which approximates an infinite plate. Thus,

$$f(a_o) = K_{Tc}^2(a_o)^{-2/(2+\omega)} \tag{A15}$$

$$f'(a_o) = -\frac{2}{2 + \omega}\frac{f(a_o)}{a_o} \tag{A16}$$

## REFERENCES


1. Kuhn, Paul: Strength Calculations for Sheet-Metal Parts with Cracks. Mater. Res. Stand., vol. 8, no. 9, Sep. 1968, pp. 21-26.

2. Orange, Thomas W.: A Semiempirical Fracture Analysis for Small Surface Cracks. NASA TN D-5340, 1969. Also Eng. Fract. Mech., vol. 3, no. 1, July 1971, pp. 53-69.

3. Feddersen, C. E.: Evaluation and Prediction of the Residual Strength of Center Cracked Tension Panels. Damage Tolerance in Aircraft Structures, Am. Soc. Test. Mater. Spec. Tech. Publ. 486, 1971, pp. 50-78.

4. Newman, J. C., Jr.: Fracture Analysis of Surface- and Through-Cracked Sheets and Plates. Eng. Fract. Mech., vol. 5, no. 3, Sept. 1973, pp. 667-689.

5. Bockrath, G. E.; and Glassco, J. B.: A Theory of Ductile Fracture. MDC-G2895, McDonnell Douglas Astronautics Co., Revised Apr. 1974.

6. Heyer, R. H.: Crack Growth Resistance Curves (R-Curves) - Literature Review. Fracture Toughness Evaluation by R-Curve Methods, Am. Soc. Test. Mater. Spec. Tech. Publ. 527, 1973, pp. 3-16.

7. Brown, W. F.; and Srawley, J. E.: Plane Strain Crack Toughness Testing of High Strength Metallic Materials. Am. Soc. Test. Mater. Spec. Tech. Publ. 410, 1966, Discussion by C. E. Feddersen, pp. 77-79.

8. Srawley, John E.: Wide Range Stress Intensity Factor Expressions for ASTM E 399 Standard Fracture Toughness Specimens. Int. J. Fract., vol. 12, no. 3, June 1976, pp. 475-476.

9. Broek, D.: The Effect of Finite Specimen Width on the Residual Strength of Light Alloy Sheet. NLR-TR-M.2152, National Lucht-en Ruimtevaartlaboratorium, Amsterdam (Netherlands), 1965.

10. Orange, Thomas W.: Fracture Toughness of Wide 2014-T6 Aluminum Sheet at $-320^{\circ}$ F. NASA TN D-4017, 1967.

11. Feddersen, C. E.; and Hyler, W. S.: Fracture and Fatigue-Crack Propagation Characteristics of 7075-T7351 Aluminum Alloy Sheet and Plate. G-8902, Battelle Memorial Inst., 1970.

12. Tada, H.; Paris, P.; and Irwin, G.: The Stress Analysis of Cracks Handbook. Del Research Corporation, 1973.

13. Kaufman, J. G.; and Nelson, F. G.: More on Specimen Size Effects in Fracture Toughness Testing. Fracture Toughness and Slow-Stable Cracking, Am. Soc. Test. Mater. Spec. Tech. Publ. 559, 1974, pp. 74-85.

14. Newman, J. C., Jr.: Crack-Opening Displacements in Center-Crack, Compact, and Crack-Line Wedge-Loaded Specimens. NASA TN D-8268, 1976.

15. Newman, J. C., Jr.: Fracture Analysis of Various Cracked Configurations in Sheet and Plate Materials. Properties Related to Fracture Toughness, Am. Soc. Test. Mater. Spec. Tech. Publ 605, 1976, pp. 104-123.

TABLE I. - PSEUDOTEST DATA FOR HYPOTHETICAL MATERIAL UNOBTAINIUM

AND FITTED EMPIRICAL PARAMETERS

(a) Annealed condition; ultimate tensile strength $\sigma_u = 150$

| $a_o$ | Center crack specimens | | | | | | Compact specimens ($a_o = 0.5$ W) | | |
|---|---|---|---|---|---|---|---|---|---|
| | W = ∞ | | W = 8.8 | | W = 4.4 | | | | |
| | $\Delta_c$ | $\sigma_c$ | $\Delta_c$ | $\sigma_c$ | $\Delta_c$ | $\sigma_c$ | W | $\Delta_c$ | $\sigma_c$ |
| 0.10 | 0.0980 | 112.56 | 0.0971 | 112.42 | 0.0945 | 112.00 | 1.5 | 0.1031 | 6.073 |
| .21 | .2015 | 93.25 | .1939 | 92.75 | .1757 | 91.36 | 3.0 | .2044 | 5.094 |
| .32 | .3008 | 83.70 | .2773 | 82.71 | .2313 | 80.08 | 4.5 | .3037 | 4.591 |
| .44 | .4044 | 77.08 | .3529 | 75.43 | .2692 | 71.29 | 6.0 | .4012 | 4.261 |
| .56 | .5036 | 72.36 | .4137 | 69.98 | .2901 | 64.26 | 7.5 | .4969 | 4.019 |
| .80 | .6897 | 65.82 | .4996 | 61.79 | .2986 | 52.84 | 11.0 | .7126 | 3.630 |
| 1.10 | .9016 | 60.36 | .5580 | 54.09 | .2713 | 41.02 | 14.0 | .8893 | 3.400 |
| $\bar{C}_m$ | 1.355 | | Not computed | | | | | | |
| $\bar{K}_u$ | 111.8 | | | | | | | | |
| $\bar{K}_{Tc}$ | 62.13 | | 60.76 | | 59.52 | | | | |
| $\bar{\omega}$ | 1.853 | | 1.727 | | 1.642 | | | | |
| $\bar{K}_f$ | 165.7 | | 172.8 | | 159.6 | | 157.7 | | |
| $\bar{m}$ | 0.8549 | | 0.8497 | | 0.7800 | | 1.0 | | |

(b) Aged condition; ultimate tensile strength $\sigma_u = 200$

| $a_o$ | Center crack specimens | | | | | | Compact specimens ($a_o = 0.5$ W) | | |
|---|---|---|---|---|---|---|---|---|---|
| | W = ∞ | | W = 96 | | W = 48 | | | | |
| | $\Delta_c$ | $\sigma_c$ | $\Delta_c$ | $\sigma_c$ | $\Delta_c$ | $\sigma_c$ | W | $\Delta_c$ | $\sigma_c$ |
| 0.05 | 0.0953 | 162.93 | 0.0953 | 162.93 | 0.0953 | 162.92 | 1.2 | 0.1011 | 8.006 |
| .36 | .2014 | 100.08 | .2014 | 100.07 | .2013 | 100.05 | 4.0 | .2049 | 5.864 |
| 1.0 | .3067 | 69.77 | .3064 | 69.74 | .3055 | 69.64 | 8.0 | .2943 | 4.592 |
| 2.0 | .4135 | 52.91 | .4121 | 52.82 | .4081 | 52.58 | 15.0 | .4042 | 3.579 |
| 3.2 | .5093 | 43.37 | .5054 | 43.21 | .4942 | 42.73 | 23.0 | .5001 | 2.988 |
| 6.4 | .6978 | 31.93 | .6791 | 31.50 | .6286 | 30.21 | 45.0 | .6971 | 2.221 |
| 12.0 | .9346 | 23.95 | .8566 | 22.87 | .6760 | 19.60 | 75.0 | .8971 | 1.759 |
| $\bar{C}_m$ | 1.820 | | Not computed | | | | | | |
| $\bar{K}_u$ | 140.7 | | | | | | | | |
| $\bar{K}_{Tc}$ | 63.80 | | 66.57 | | 68.38 | | | | |
| $\bar{\omega}$ | 0.838 | | 1.151 | | 1.310 | | | | |
| $\bar{K}_f$ | 163.3 | | 166.0 | | 168.4 | | 167.0 | | |
| $\bar{m}$ | 0.7266 | | 0.7378 | | 0.7469 | | 0.9533 | | |

TABLE II. - EMPIRICAL PARAMETERS FOR TEST DATA FROM THE LITERATURE

| Data source | Alloy | Specimen constant | Empirical parameters (ref. 4) | | | Empirical parameters (ref. 5)[a] | | |
|---|---|---|---|---|---|---|---|---|
| | | | $K_f$ | | m | $K_{Tc}$ | | $\omega$ |
| | | | $MN\text{-}m^{-3/2}$ | $ksi\sqrt{in.}$ | | $MN\text{-}m^{-1.761}$ | $lb\text{-}in.^{-1.761}$ | |
| Ref. 10 | 2014-T6 | W = 30 cm | 89.9 | 81.8 | 0.8094 | 99.70 | 34 790 | 2.188 |
| Ref. 11 | 7075-T7351 | W = 40 cm | 84.1 | 76.5 | 1.0 | | | |
| Ref. 13 | 2219-T851 | B = 13 mm | 101.4 | 92.3 | 1.0 | | | |
| | | B = 25 mm | 78.2 | 71.1 | 1.0 | | | |
| | | B = 38 mm | 65.4 | 59.5 | .8921 | Not computed | | |
| | | B = 50 mm | 58.4 | 53.1 | .6997 | | | |
| Ref. 1 | 2219-T87 | W = 60 cm | 183.1 | 166.6 | 0.8841 | | | |
| | | W = 120 cm | 210.2 | 191.3 | 1.0 | | | |

[a]Only specimens having $a_o \leq W/20$ were included in least squares fit.

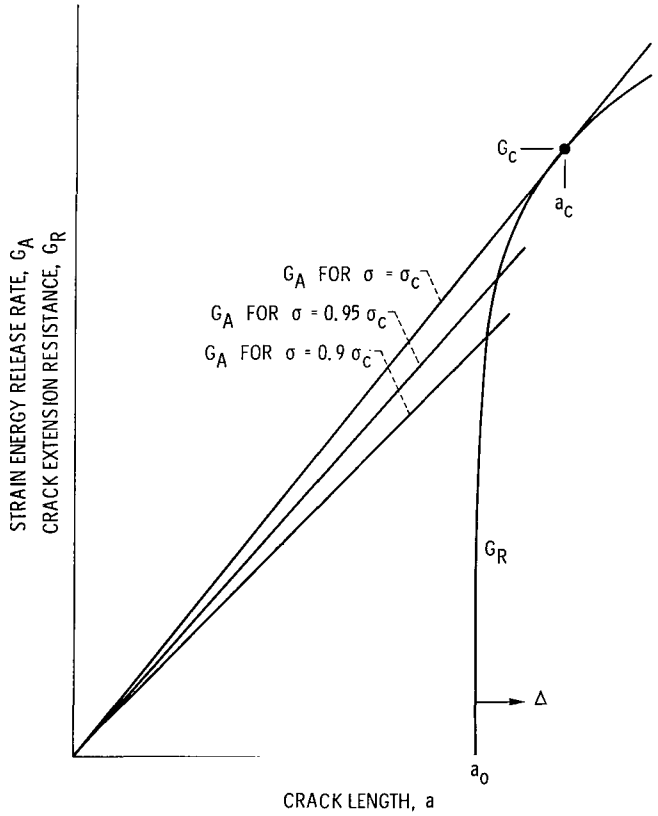


Figure 1. - Schematic representation of R-curve instability concept for an infinite body.

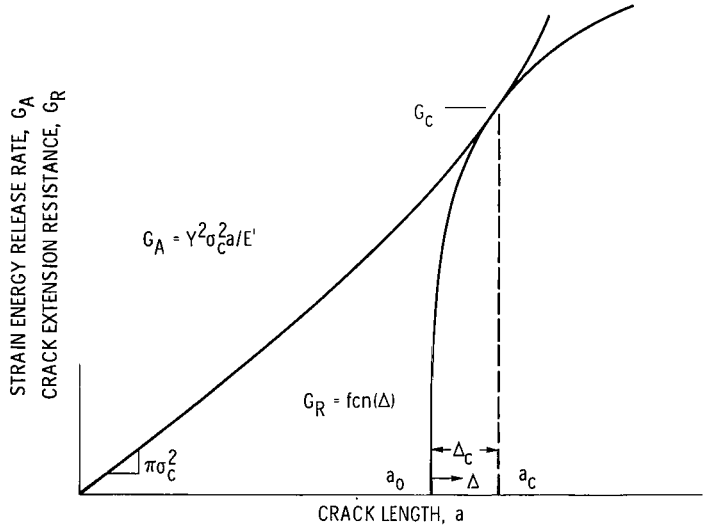


Figure 2. - R-curve instability concept for a finite body.

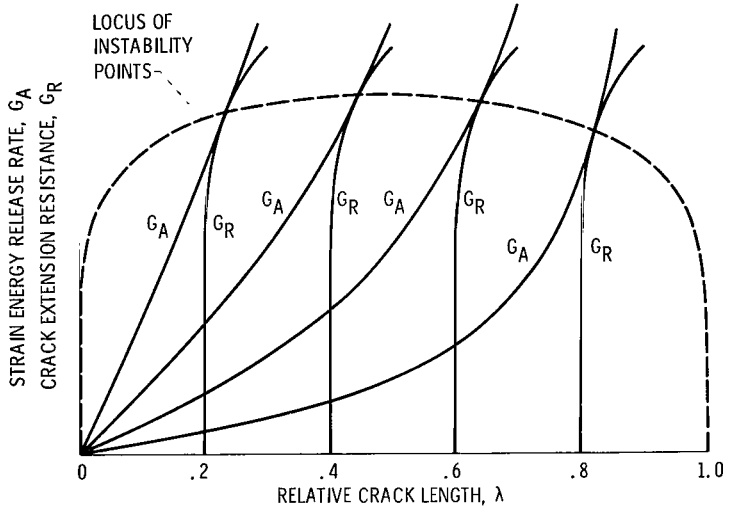


Figure 3. - R-curve instability for a wide range of initial crack lengths.

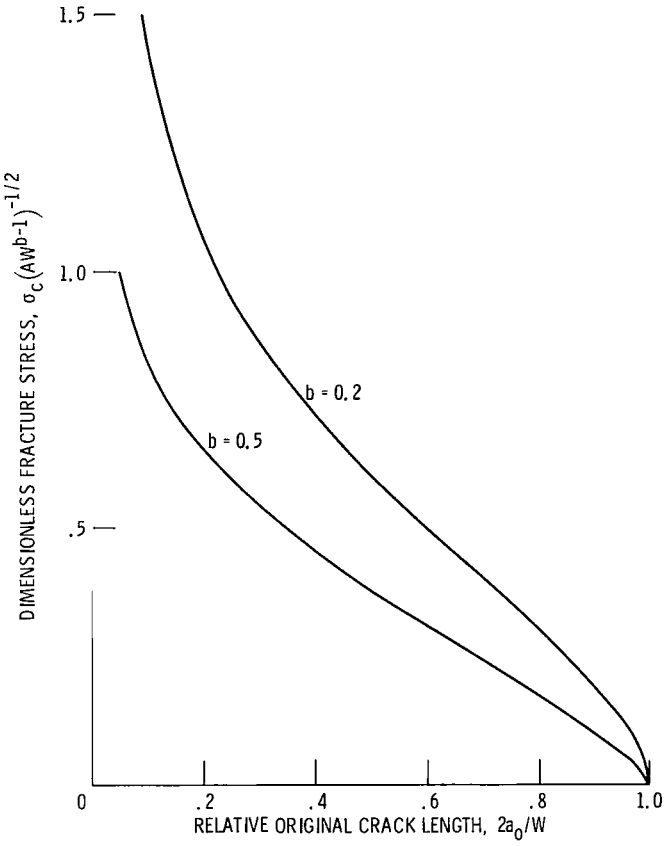


Figure 4. - Dimensionless residual strength for center-crack specimens of a material with an R-curve of the general form $E'G_R = A(\Delta)^b$.

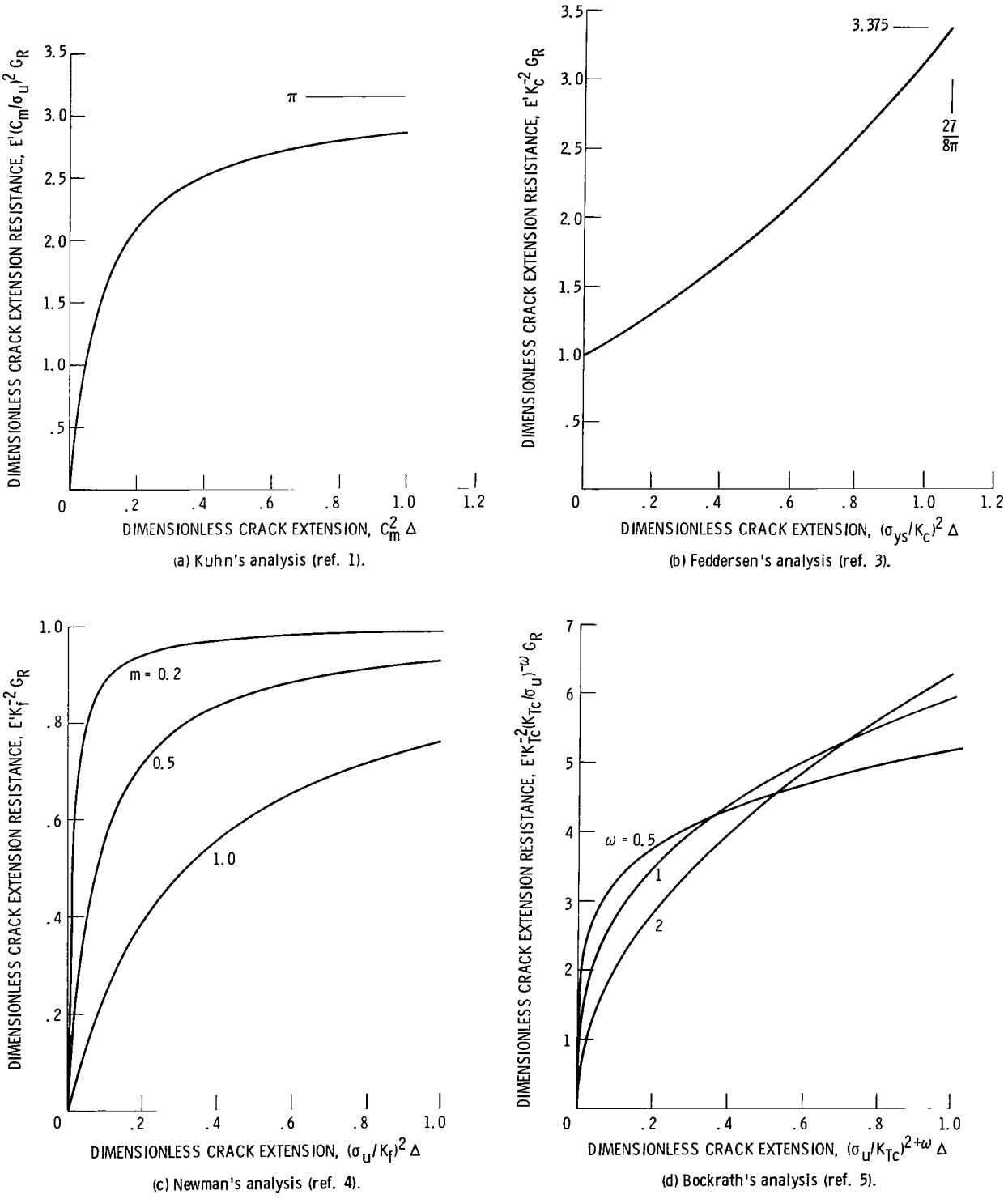


Figure 5. - Dimensionless R-curves equivalent to various semiempirical fracture analyses for the case of a crack in an infinite plate.

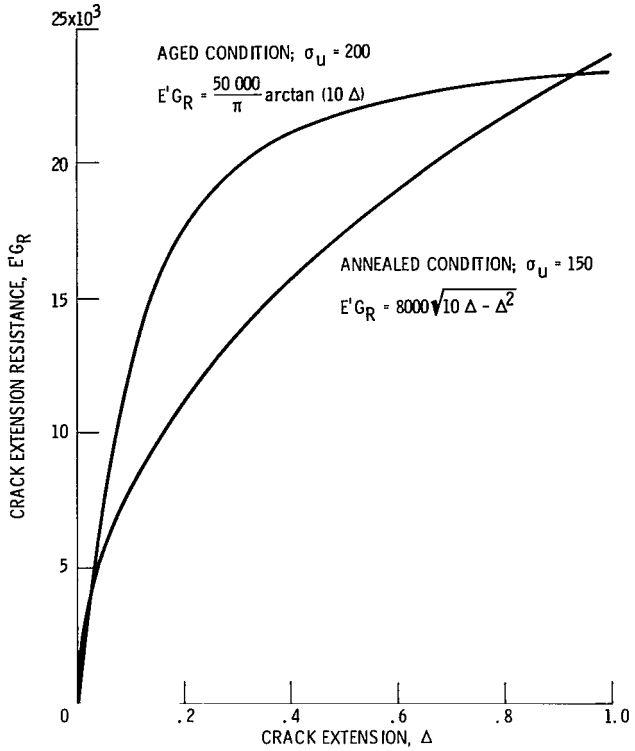


Figure 6. - R-curves for hypothetical material Unobtanium.

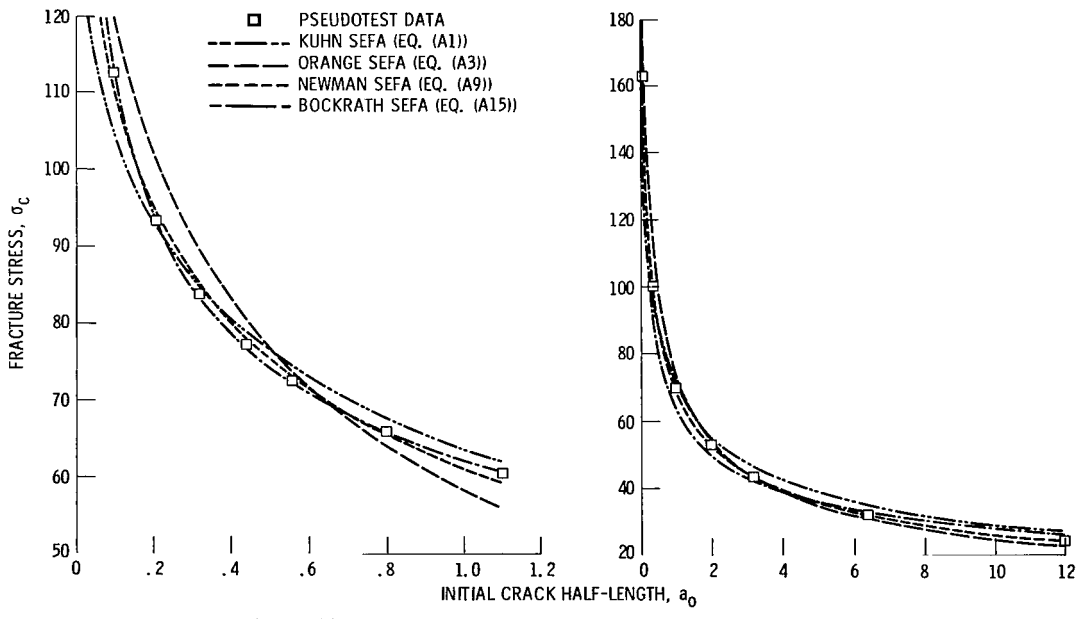


(a) Annealed condition: $\sigma_U = 150$. (b) Aged condition: $\sigma_U = 200$.

Figure 7. - Residual strength of hypothetical material Unobtainium, infinite width series; various semiempirical fracture analysis (SEFA) fit to pseudotest data.

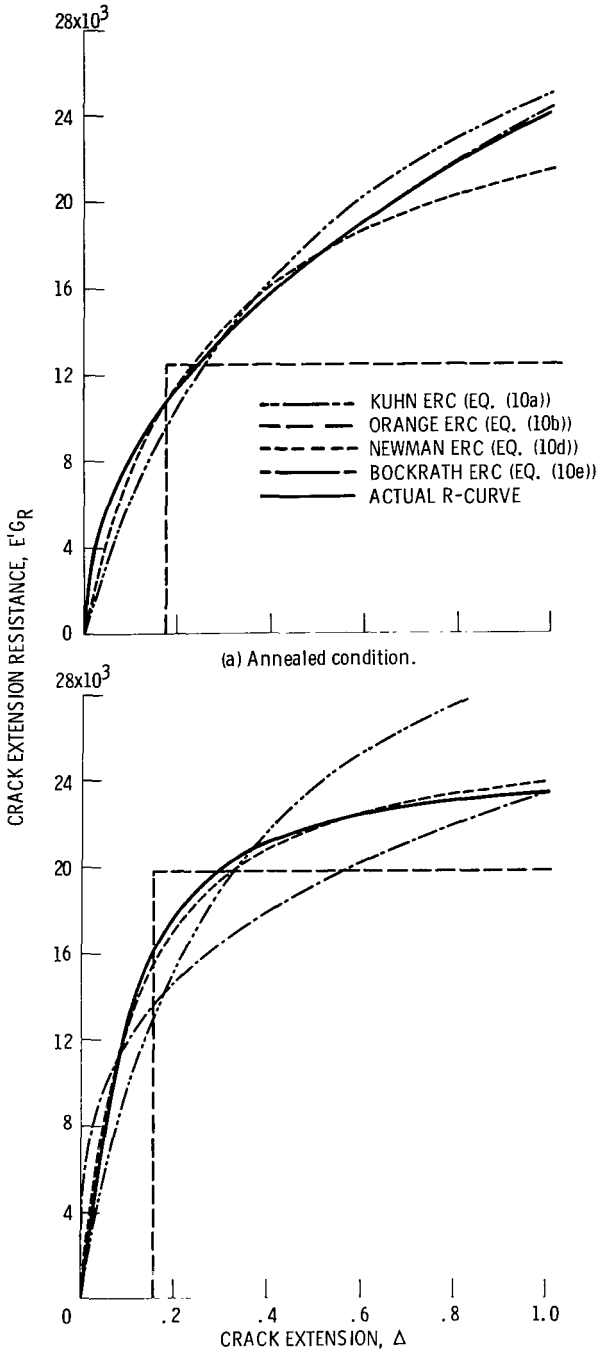


Figure 8. - Actual R-curves and equivalent R-curves (ERC) for hypothetical material Unobtainium; infinite-width series.

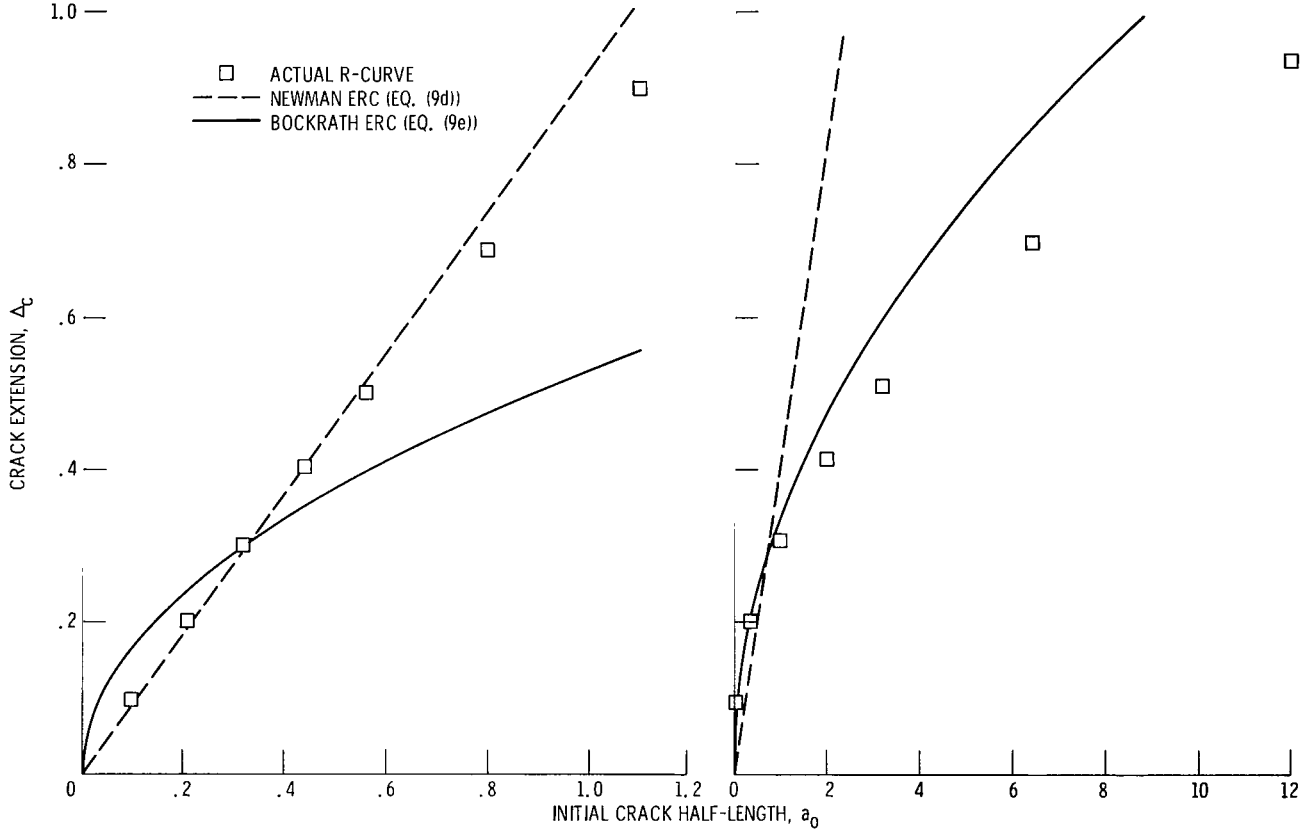


(a) Annealed condition.

(b) Aged condition.

Figure 9. - Critical crack extension for hypothetical material Unobtainium; infinite width series; calculated from actual R-curves and from equivalent R-curves (ERC).

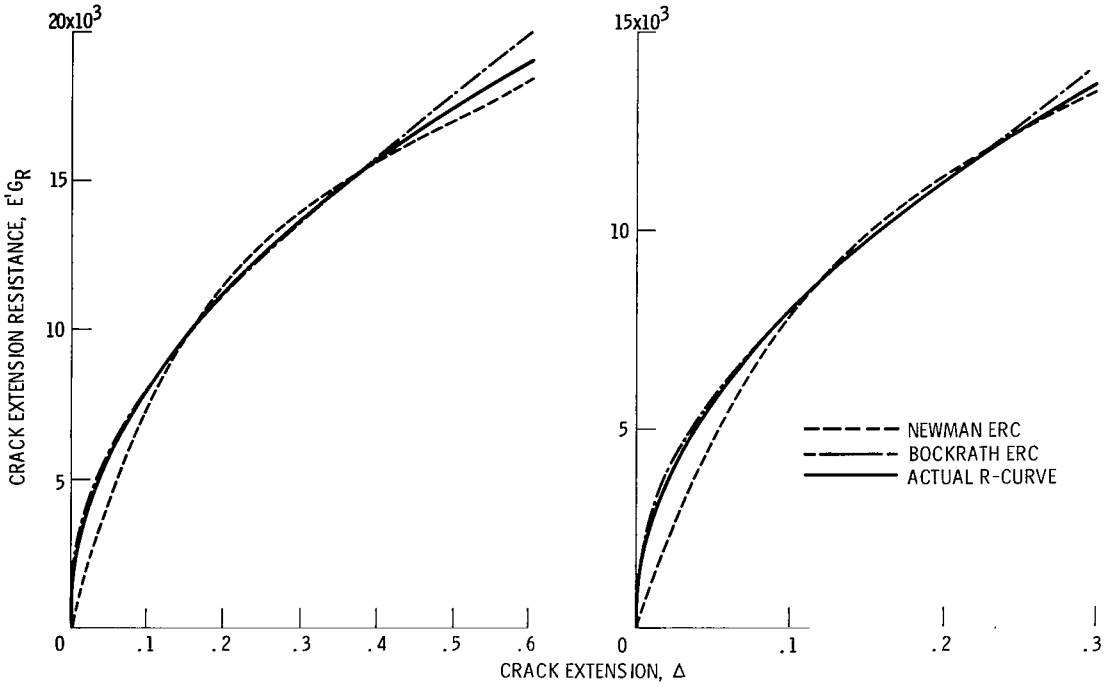


(a) Width W = 8.8.

(b) Width W = 4.4.

Figure 10. - Actual R-curve and equivalent R-curves (ERC) for hypothetical material Unobtainium; finite width; annealed condition.

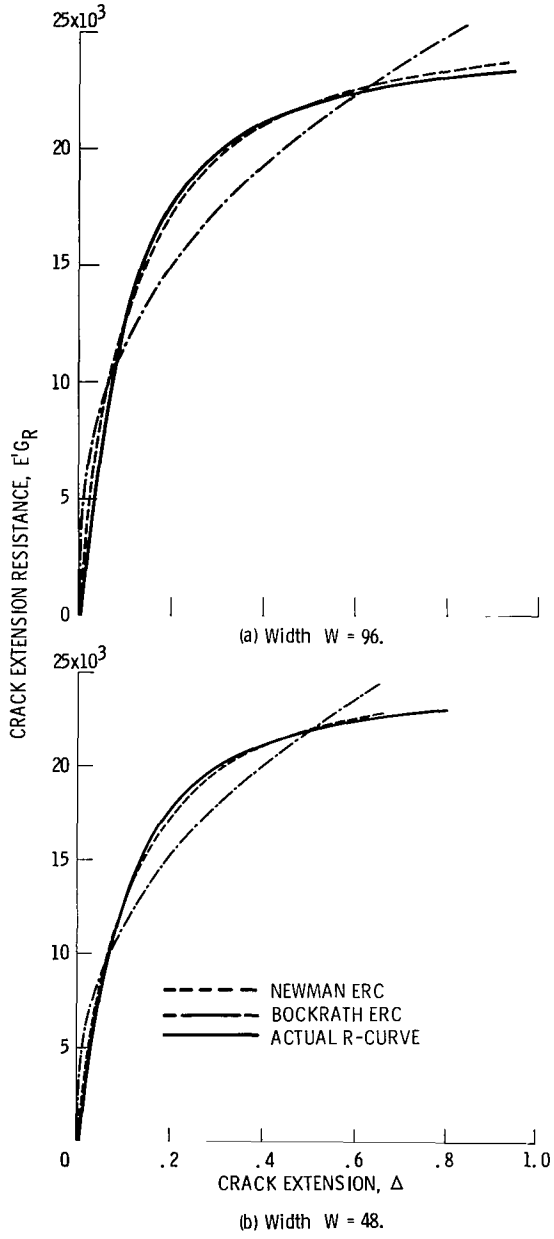


Figure 11. - Actual R-curve and equivalent R-curves (ERC) for hypothetical material Unobtainium; finite width; aged condition.

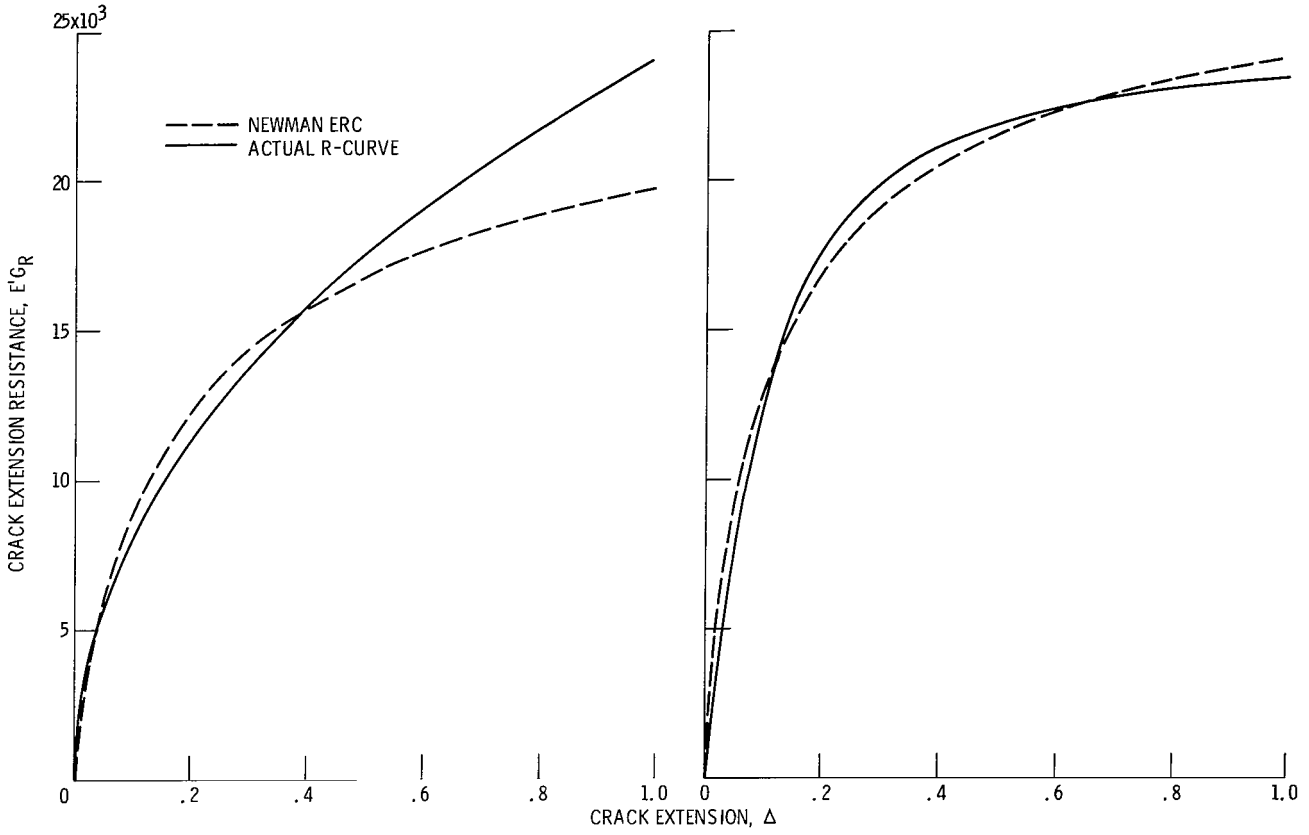


(a) Annealed condition.

(b) Aged condition.

Figure 12. - Actual R-curves and equivalent R-curves (ERC) for hypothetical material Unobtainium; compact specimens; $a_0/W = 0.5$.

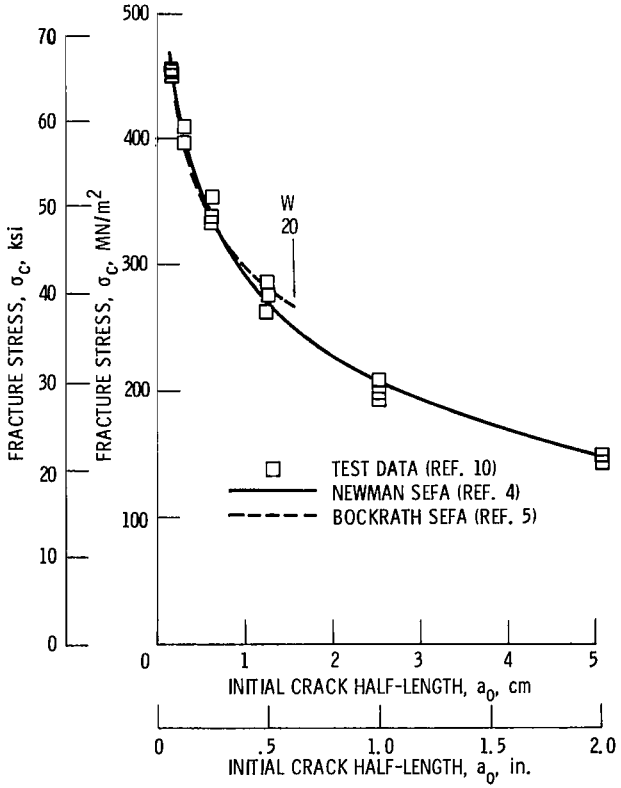


Figure 13. - Residual strength of 2014-T6 aluminum alloy sheet at 77 K (ref. 10); two semiempirical fracture analyses (SEFA) fit to test data.

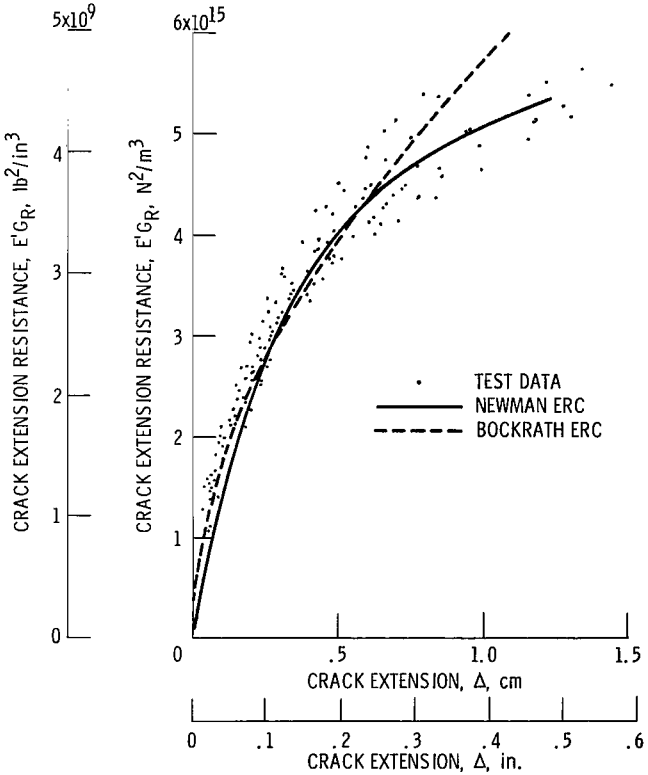


Figure 14. - Equivalent R-curves (ERC) and test data points for 2014-T6 aluminum alloy sheet at 77 K (ref. 10).

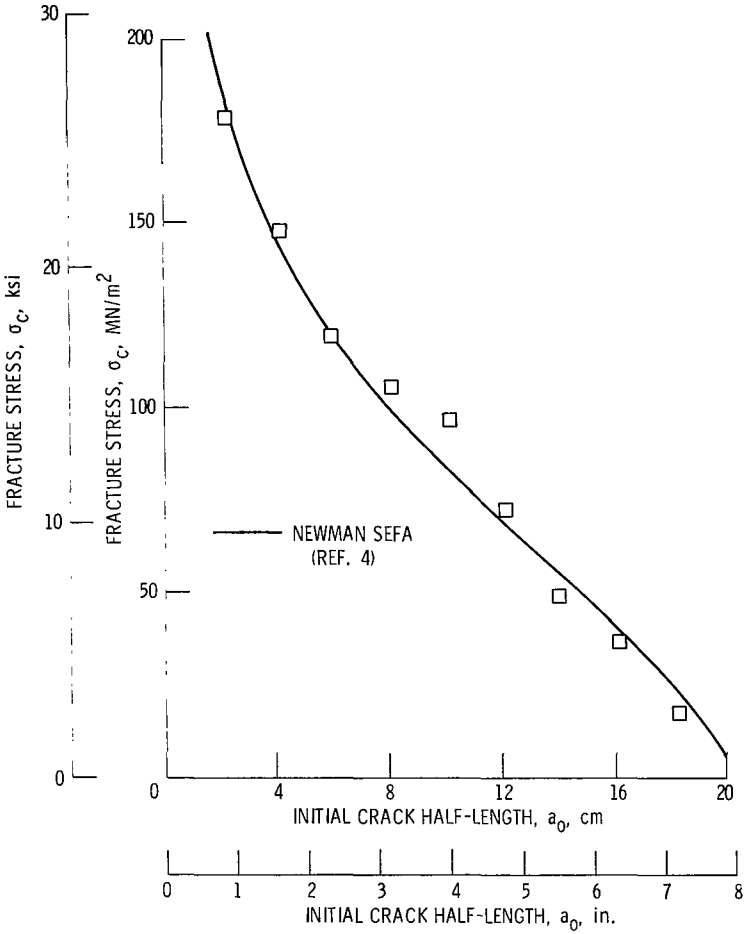


Figure 15. - Residual strength of 7075-T7351 aluminum alloy plate (ref. 11); Newman's semiempirical fracture analysis (SEFA) fit to test data.

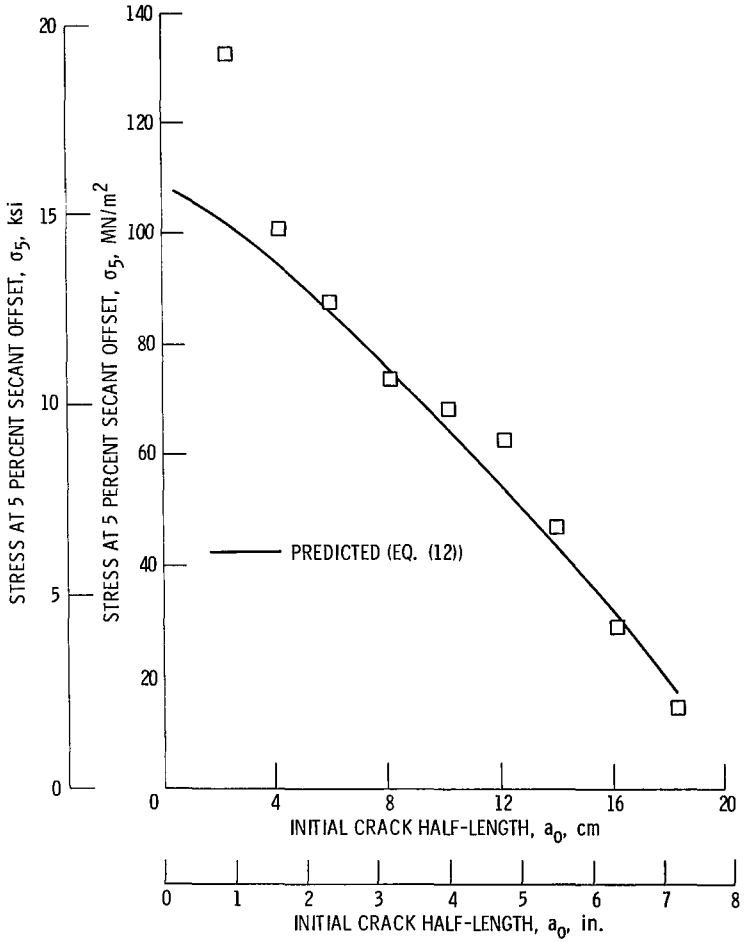


Figure 16. - Stress at 5 percent secant offset $\sigma_5$ for data from reference 11, predicted using equation (12).

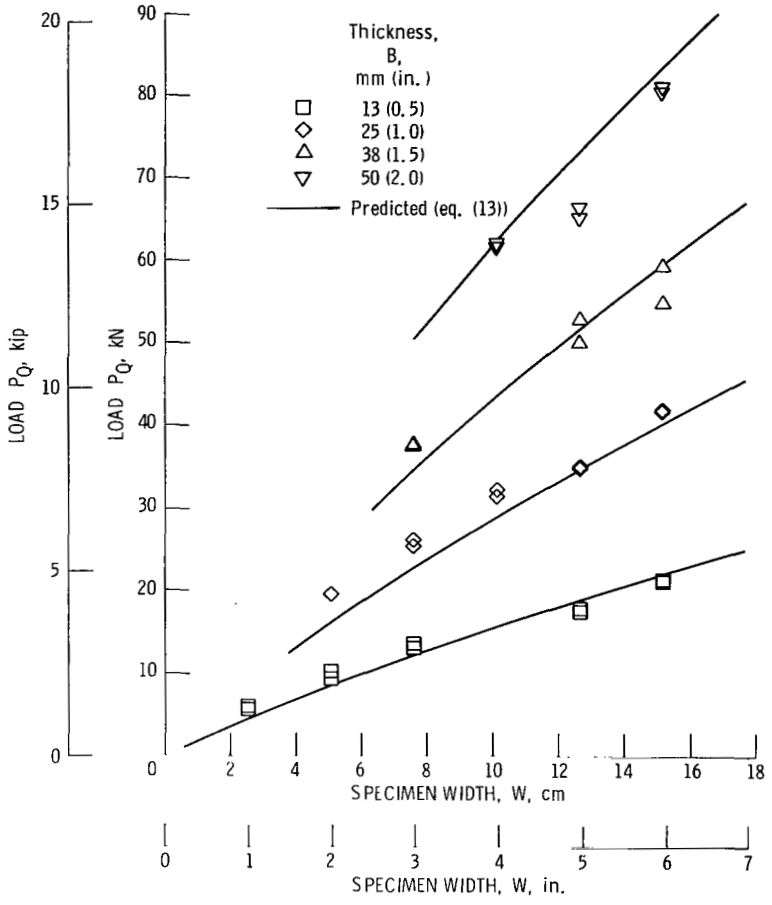


Figure 17. - Load at 5 percent secant offset $P_Q$ for 2219-T851 aluminum alloy compact specimens (ref. 13), predicted from Newman equivalent R-curve.

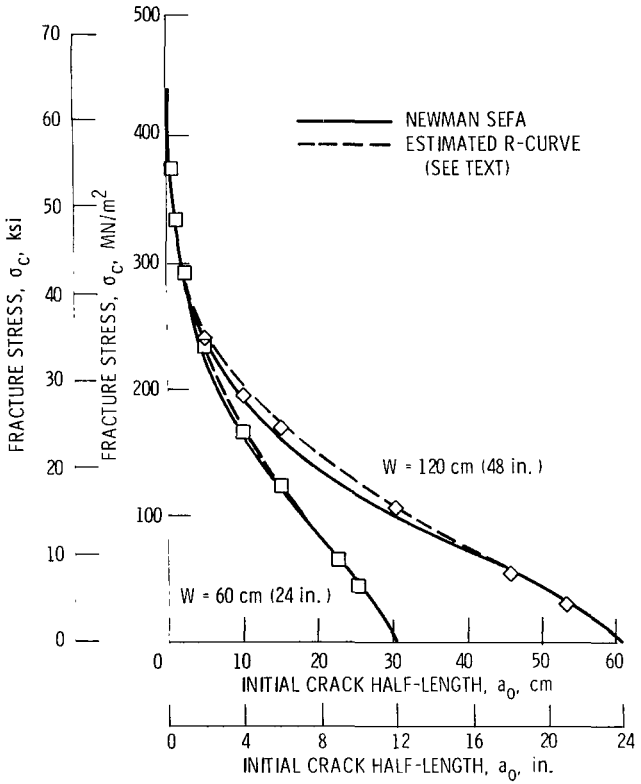


Figure 18. - Residual strength of 2219-T87 aluminum alloy sheet (ref. 1) calculated from Newman's semiempirical fracture analysis (SEFA) and from estimated R-curve.

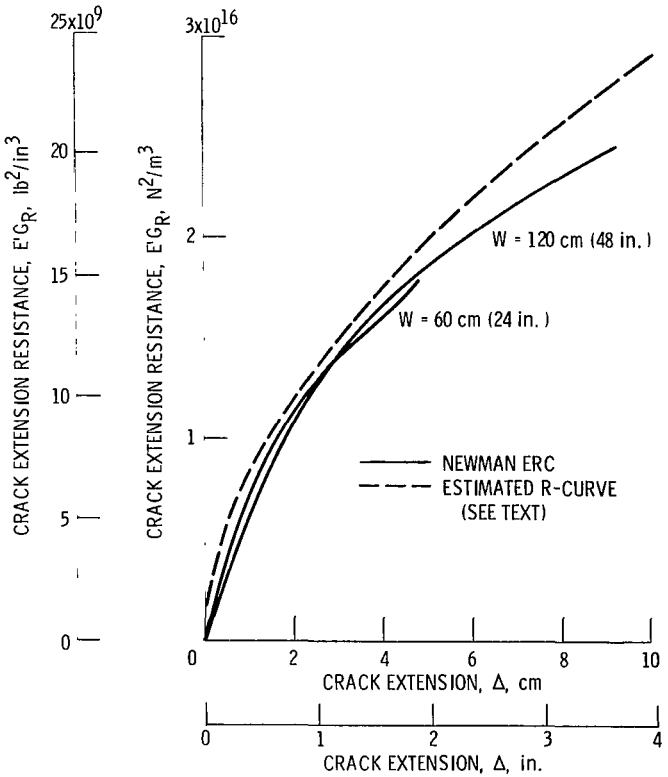


Figure 19. - Equivalent R-curves (ERC) and estimated R-curve for 2219-T87 aluminum alloy sheet (ref. 1).

| 1. Report No. | 2. Government Accession No. | 3. Recipient's Catalog No. |
|---|---|---|
| NASA TP-1600 | | |

4. Title and Subtitle

A RELATION BETWEEN SEMIEMPIRICAL FRACTURE ANALYSES AND R-CURVES

5. Report Date: January 1980

6. Performing Organization Code

7. Author(s): Thomas W. Orange

8. Performing Organization Report No.: E-9963

9. Performing Organization Name and Address
National Aeronautics and Space Administration
Lewis Research Center
Cleveland, Ohio 44135

10. Work Unit No.: 505-02

11. Contract or Grant No.

12. Sponsoring Agency Name and Address
National Aeronautics and Space Administration
Washington, D.C. 20546

13. Type of Report and Period Covered: Technical Paper

14. Sponsoring Agency Code

15. Supplementary Notes

16. Abstract

The relations between several semiempirical fracture analyses (SEFA) and the R-curve concept of fracture mechanics are examined and the conditions for equivalence between a SEFA and an R-curve are derived. A hypothetical material is employed to study the relation analytically. Equivalent R-curves are developed for several real materials using data from the literature. For each SEFA there is an equivalent R-curve whose magnitude and shape are determined by the SEFA formulation and its empirical parameters. If the R-curve is indeed unique, then the various empirical parameters cannot be constant, and vice versa. However, for one SEFA the differences are small enough that they may be within the range of normal data scatter for real materials.

| 17. Key Words (Suggested by Author(s)) | 18. Distribution Statement |
|---|---|
| Cracks; Crack growth; Fracture mechanics; Fracture properties; Resistance curves; Residual strength; Semiempirical analyses | Unclassified - unlimited<br>STAR Category 39 |

| 19. Security Classif. (of this report) | 20. Security Classif. (of this page) | 21. No. of Pages | 22. Price* |
|---|---|---|---|
| Unclassified | Unclassified | 44 | A03 |

* For sale by the National Technical Information Service, Springfield, Virginia 22161

NASA-Langley, 1980

6 1 1U,D, 122179 S00903DS
DEPT OF THE AIR FORCE
AF WEAPONS LABORATORY
ATTN: TECHNICAL LIBRARY (SUL)
KIRTLAND AFB NM 87117

S